Tetramethyleneethane (TME) Diradical: Experiment and Density Functional Theory Reach an Agreement

Michael Filatov* and Sason Shaik

Department of Organic Chemistry and The Lise Meitner-Minerva Center for Computational Quantum Chemistry, The Hebrew University of Jerusalem, 91904 Jerusalem, Israel

Received: June 21, 1999; In Final Form: August 26, 1999

REKS-type (Filatov, M.; Shaik, S. *Chem. Phys. Lett.* **1999**, *304*, 429) density functional calculations were carried out for the lowest energy singlet and triplet states of tetramethyleneethane (TME) diradical. The calculations indicate that the ground state of TME in the gas phase is the singlet state, whereas the triplet state should be metastable at low temperatures. The triplet state metastability derives from the energetic preference for the triplet state at the optimal triplet molecular geometry and from the extremely small (<0.05 cm^{-1}) spin−orbit coupling between the triplet and ground singlet states. REKS calculations predict that, in the vibrational spectra of the two states of TME, the modes corresponding to symmetric scissoring vibrations should have nearly the same frequencies of 357 cm^{-1}, in accord with the experimental observation of two modes of the same frequency of 335 cm^{-1} in the vibrational structure of the photoelectron spectrum of the $[TME]^-$ anion.

1. Introduction

Tetramethyleneethane[1,2] (TME) **1** is the simplest representative of disjoint diradicals.[3−5] The two frontier orbitals of TME are very close in energy and thus the lowest electronic states of TME, one singlet and one triplet, are nearly degenerate.[6−8] The identity of TME's ground state has long been a subject of controversy between experiment[1,2] and theory.[3−8] Matrix isolation ESR experiment[2] yielded a linear Curie−Weiss plot, thereby indicating that either the ground state of TME is triplet or that the triplet and singlet states are degenerate. However, this conclusion has been challenged by ab initio (6,6)CASSCF/3-21G[7] and two reference SD-CI/DZP[6] calculations which place the singlet state ca. 1−1.5 kcal/mol below the triplet. Later, theory and experiment seemed to reconcile, when two reference SD-CI/TZ2P calculations[8] on (6,6)CASSCF/3-21G geometries[7] predicted that the minimum on the triplet state potential energy surface of TME lies ca. 0.1 kcal/mol below the respective singlet state minimum.

However, recently the controversy flared again when negative ion photoelectron spectroscopy[9] of $[TME]^-$ anion revealed that the ground state of TME in gas phase is a singlet state with the triplet state lying ca. 2 kcal/mol above. Furthermore, it was experimentally detected[9] that upon photodetachment of electron from $[TME]^-$ anion two vibrational modes, each with frequency of 335 cm^{-1}, are excited in the two states of the neutral TME. Unfortunately, ab initio calculations[9] did not yield equal frequencies for the suspected modes in vibrational spectra of the two states, thereby increasing the disagreement between theory and experiment.

These gas-phase results[9] appear to be inconsistent with earlier ESR matrix isolation studies.[2] To settle this problem it was assumed[9] that the triplet state of TME isolated in glass matrices at low temperatures is metastable and undergoes a slow relaxation to the ground singlet state. However, the spin−orbit matrix elements which couple singlet and triplet states were not calculated to substantiate this scenario.

In previous theoretical studies[6−8] of TME, it was the standard practice to optimize molecular geometry and calculate vibrational frequencies either at the Hartree−Fock level[6] or at computational levels with electron correlation limited to the π-electrons (max six electrons in six active π-type orbitals).[7−9] Dynamic correlation effects between σ- and π-type electrons, which are important for adequate description of the electronic and molecular structure of diradicals,[10] were included at the CI level[6,8] employing the molecular structures from the lower level calculations. It is possible that had the dynamic correlation effects been included from the very beginning, the optimized molecular structures, the singlet−triplet energy gaps and the vibrational frequencies, would have changed significantly.[10] Unfortunately, geometry optimizations and vibrational analyses by the conventional multireference ab initio methods are still too costly even for molecules of moderate size.

Density functional theory[11−13] is an inexpensive alternative to the conventional quantum chemical methods in studies of big systems. While modern approximate density functionals simulate quite well[14] dynamic many-particle correlations, they are less successful[15−17] in accounting for nondynamic correlation due to degeneracy or near-degeneracy of several electronic configurations. Thus, one cannot obtain reliable energetic and structural properties of diradicaloid species from the standard density functional calculations.[17−19]

Recently, we have developed[20] a Kohn−Sham-type density functional method suited for treating the nondynamic electron correlation in diradicals. In this method, called spin-restricted ensemble-referenced Kohn−Sham (REKS) method, the energy and the density of a state with strong nondynamic correlation are represented[20] as weighted sums (ensembles) of several symmetry-adapted Kohn−Sham (KS) determinants.[11,12] The REKS method has been tested[20] on a number of diradicaloid species and has yielded results of essentially the same quality as provided by conventional multireference methods (MRD-CI, CASSCF, etc.).

10.1021/jp9920489 CCC: $18.00
Published on Web 10/21/1999

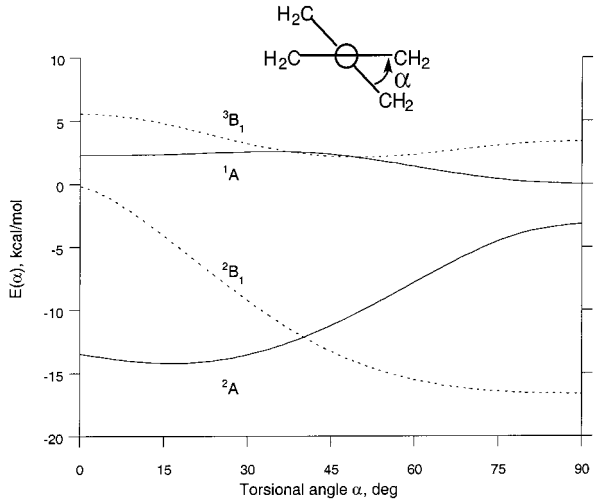

Figure 1. Density functional energies of the $^3B_1$ and ^1A states of TME and $^2B_1$ and ^2A states of $[TME]^-$ as functions of torsional angle α. The energy of the ^1A state is used as origin of energy scale (−233.26908 hartree).

The present paper applies the REKS method to study the electronic and molecular structure of the lowest singlet and triplet states of TME. The key to singlet−triplet interconversion in TME is the torsional motion of the two allylic fragments about the central C−C bond.[6−9] On the basis of density functional calculations of the dependence of the energies of singlet and triplet states on the torsion angle, it is demonstrated that the singlet is indeed the ground state in gas phase. In addition, it is shown that the triplet TME which is observed in matrix isolation experiments should be metastable at low temperatures due to the fact that at optimal triplet molecular geometry the triplet state is below the singlet, as well as due to extremely small spin−orbit coupling (<0.05 cm^{-1}) between the two spin states.

2. Details of Calculations

All density functional and CASSCF calculations employed the 6-311G** basis set[21] and were performed at a D_2 symmetry. The potential energy curves along the twisting mode α (see Figure 1 for definition) were calculated for the singlet ^1A and triplet $^3B_1$ states of neutral TME. Density functional calculations were also performed for the ^2A and $^2B_1$ states of $[TME]^-$ anion. Calculations of twisting potential energy curves were done for a number of twisting angles in the interval 0°−90°, while optimizing simultaneously all other geometric parameters under the D_2 symmetry constraint.

The symmetry-adapted spin-restricted open-shell Kohn−Sham (ROKS) method[22,23] was employed for the triplet and doublet states. The spin-restricted ensemble-referenced Kohn−Sham (REKS) method[20] was used to calculate the singlet states. The singly occupied one-electron orbitals in the $^3B_1$ state belong to b_1 and a irreducible representations in the D_2 symmetry group (see Scheme 1). In the REKS calculations, the $6b_1$ and $7a$ orbitals were fractionally occupied and their occupation numbers were optimized simultaneously along with the one-electron orbitals. In the doublet $^2B_1$ and ^2A states of $[TME]^-$, the singly occupied orbitals belong to b_1 and a irreducible representations, respectively.

All density functional calculations were carried out with the local version of the CADPAC5 program[24] that implements the ROKS and REKS methods and employed the BLYP gradient-corrected density functional.[25] CASSCF and CASMP2[26,27] calculations were performed using the GAMESS-USA package[28] for the singlet and triplet states of TME based on geometries from density functional calculations. In these calculations all symmetry-allowed configurations which correlate six electrons in the six orbital active space were included. The active orbitals are the π-type orbitals of the allylic fragments shown in Scheme 1. Spin−orbit coupling calculations were carried out with the (6,6)CASSCF wave functions using an approximate one-electron spin−orbit (SO) operator with an effective nuclear charge for carbon $Z^* = 3.6$, determined previously by Koseki et al.,[29] and shown to yield compatible results with the full Breit−Pauli calculation.[30]

SCHEME 1

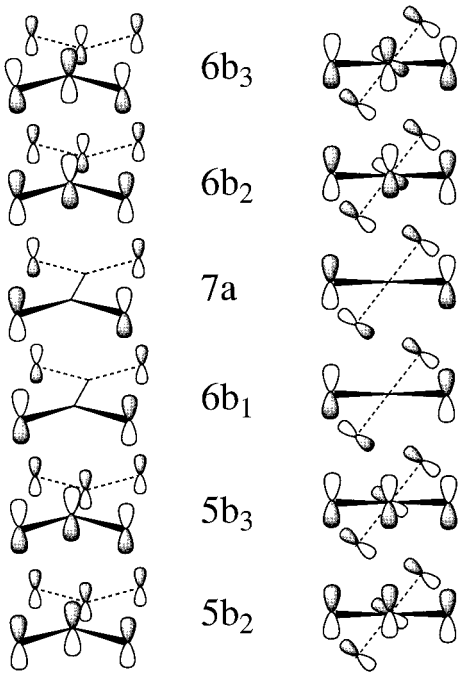

3. Results and Discussion

The results of density functional and CASMP2 calculations are summarized in Figure 1, which displays the dependence of the energies of $^3B_1$ and ^1A states of neutral TME as well as of $^2B_1$ and ^2A states of $[TME]^-$ anion.

The ROKS curve for the $^3B_1$ state of TME minimizes at angle 50.1° in good accord with previous CASSCF/3-21G[7] and B3LYP[9] calculations. The minimum on the triplet potential energy curve occurs near the point where the two singly occupied orbitals, $6b_1$ and $7a$, cross. The bonding character of the two orbitals varies with the twist angle (see Scheme 1); at a planar geometry $6b_1$ is weakly bonding and $7a$ is weakly antibonding, and vice versa at twist angles α > 40°. The orbital crossing occurs between 40° and 50° of twist, and in this region the antibonding character of one orbital is approximately compensated by the bonding character of another.

The planar (D_{2h}) and perpendicular (D_{2d}) structures on the triplet potential energy surface are saddle points connecting two mirror image minima. Steric repulsion between the two allyl fragments in TME accounts for the different heights of these two barriers. The CCC angle in allyl fragments varies from 118.5° to 122.4° (see Figure 3c), thus allowing some relief in steric repulsion, when going from the planar to the perpendicular structure.

The energy of the singlet state is minimal at 90° of twist both with REKS and CASMP2 calculations (see Figure 2). It

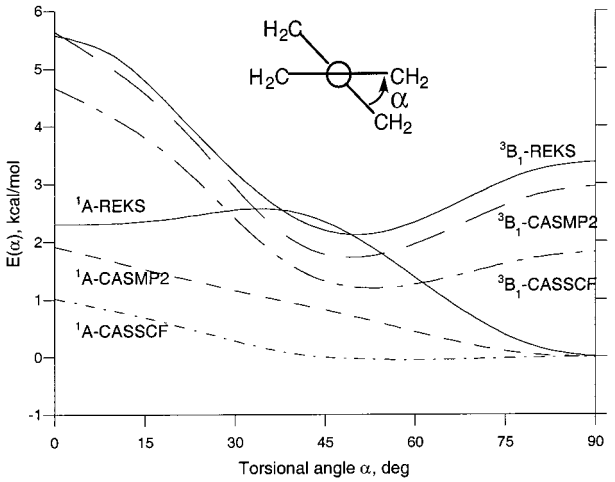

Figure 2. Energies of the $^3B_1$ and ^1A states of TME vs torsional angle α, obtained from REKS/ROKS, CASMP2, and CASSCF calculations. The energy of the ^1A state is used as origin of energy scale (−233.26908 hartree (REKS), −232.66276 hartree (CASMP2), −231.86724 hartree (CASSCF)).

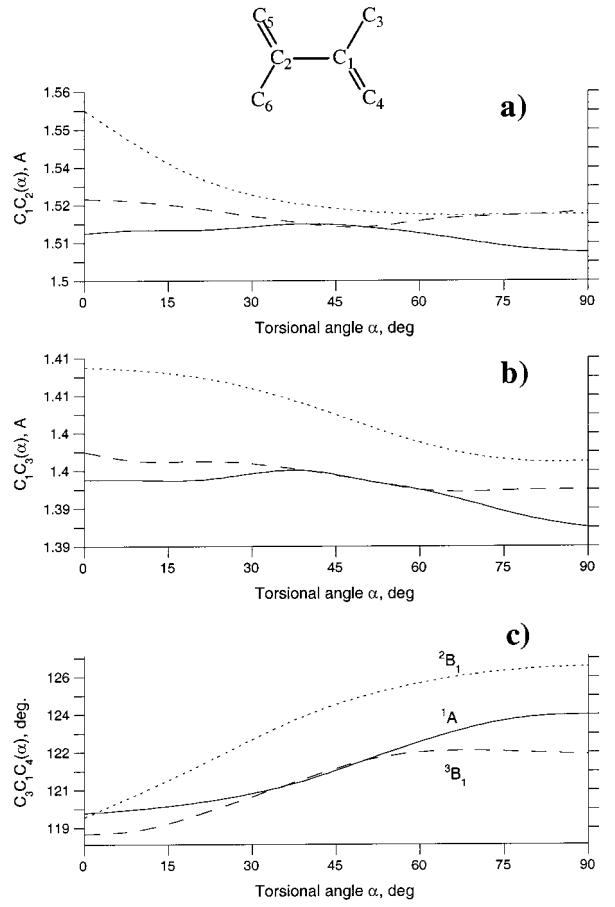

Figure 3. Optimized C_1C_2 bond lengths (a), C_1C_3 bond lengths (b), and allylic CCC angles (c) in the $^3B_1$ (dashed line) and ^1A (solid line) states of TME and in the $^2B_1$ state (dotted line) of $[TME]^-$ as functions of torsional angle α.

is interesting to note that the energy differences between planar and perpendicular structures are nearly the same for the triplet and singlet states. The REKS/ROKS calculations yield 2.2 kcal/mol (2.3 kcal/mol) for $E^{1A}(0°) - E^{1A}(90°)$ ($E^{3B1}(0°) - E^{3B1}(90°)$) and (6,6)CASMP2 yields 2.0 kcal/mol (2.7 kcal/mol), respectively. We therefore attribute this nearly constant difference to steric relief at the perpendicular geometry for both states.

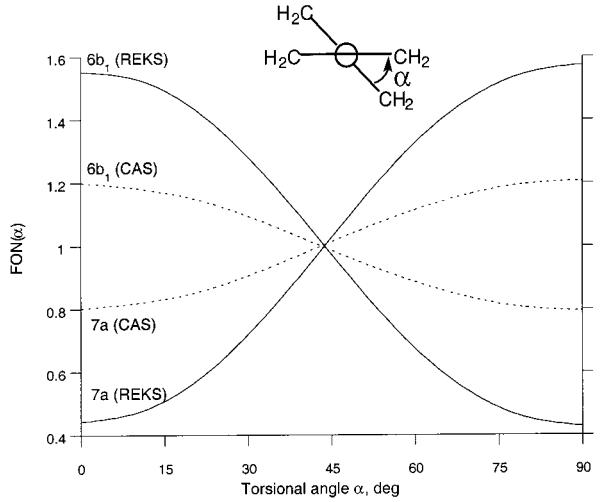

Figure 4. Fractional occupation numbers of the $6b_1$ and $7a$ orbitals (Scheme 1) from REKS calculation of singlet TME and of the corresponding natural orbitals from CASSCF calculation as functions of torsional angle α.

The bonding character of $6b_1$ and $7a$ orbitals affects less the singlet state potential energy curve, because both configurations, $(6b_1)^2$ and $(7a)^2$, contribute to the singlet state and their weights in CASSCF and REKS calculations are adjusted according to their bonding/antibonding character. Figure 4 shows the dependence on twist angle of the fractional occupation numbers of the $6b_1$ and $7a$ orbitals, as obtained in the REKS and in the corresponding CASSCF calculations. At every twist angle, the most bonding orbital is more populated. The populations of the two active orbitals become nearly equal in the region between 40° and 50° of twist, the locus of orbital crossing.

In disjoint diradicals, the fractionally occupied orbitals can be localized and confined to different groups of atoms in the molecule.[3−5] In the case of TME, the $6b_1$ and $7a$ orbitals can be viewed as composed from the nonbonding orbitals of the two allyl fragments, i.e., $6b_1 = (\chi_1 + \chi_2)/\sqrt{2}$ and $7a = (\chi_1 - \chi_2)/\sqrt{2}$, where the χ_1 and χ_2 are the nonbonding allylic orbitals assumed to be mutually orthogonal. Thus, the wave function of the ^1A state can be decomposed as follows:

$$\Psi(^1A) = c_1|6b_1\bar{6b}_1\rangle - c_2|7a\bar{7a}\rangle = \frac{c_1 + c_2}{\sqrt{2}}\left(\frac{1}{\sqrt{2}}\left|\chi_1\bar{\chi}_2\right\rangle + \frac{1}{\sqrt{2}}\left|\chi_2\bar{\chi}_1\right\rangle\right) + \frac{c_1 - c_2}{\sqrt{2}}\left(\frac{1}{\sqrt{2}}\left|\chi_1\bar{\chi}_1\right\rangle + \frac{1}{\sqrt{2}}\left|\chi_2\bar{\chi}_2\right\rangle\right) \quad (1)$$

The first term in eq 1 represents a purely covalent component of the wave function and the second term is ionic describing coupled $(allyl)^+(allyl)^-$ fragments. Generally, this ionic contribution stabilizes a diradicaloid state.[31,32] When $c_1 \sim c_2$, the ionic stabilization is lost and the state of the singlet diradical becomes purely covalent, like the corresponding triplet state that cannot admix an ionic contribution because of the exclusion principle. Thus, the ^1A state of TME has a mixed covalent−ionic character near the planar and perpendicular structures but is almost purely covalent in the region between 40° and 50°, where the occupation numbers of the $6b_1$ and $7a$ orbitals are nearly equal both with REKS and CASSCF calculations.

The singlet state potential curve (Figures 1 and 2) is nearly flat at torsion angles less than 40°. The REKS/BLYP/6-311G** calculation even yields a very low energy transition state at torsion angles around 40°. However, this state is only 0.2 kcal/mol above the planar structure and does not have real chemical

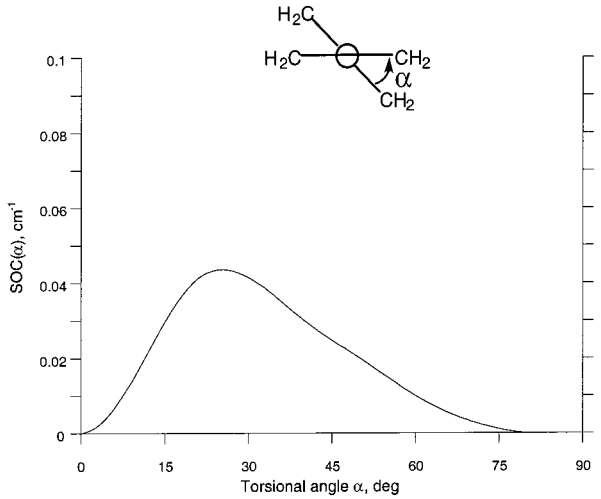

Figure 5. The spin−orbit coupling matrix element between the $^3B_1$ and ^1A states as function of torsional angle α.

significance.[33] The REKS/ROKS calculations (Figure 2) predict that at twist angles of 38° and 50°, the singlet and triplet curves cross. Between the crossing points, the singlet−triplet (S−T) energy gap is about −0.1 kcal/mol favoring the triplet state. The (6,6)CASMP2/6-311G** calculations do not yield curve crossing (S−T gap ≥ 1 kcal/mol) and the (6,6)CASSCF yields even larger S−T gap. The CASSCF predicts also a very shallow minimum on the singlet potential curve at a twist angle near 60°. The same trend was observed earlier in (6,6)CASSCF/3-21G calculations.[7] In contrast with the CASSCF and CASMP2 results, the two reference SD-CI/TZ2P calculations,[8] predict curve crossing at twist angles of ca. 30° and 60° and a more substantial singlet−triplet gap of about −1 kcal/mol in favor of the triplet state. The results of the present density functional calculations are, in principle, consistent with the two reference SD-CI and CASMP2 calculations in the sense that a realistic twist potential curve can be expected to lie between the SD-CI and CASMP2 ones.[9]

The torsional potential energy curves for the $^2B_1$ and ^2A states of TME anion are also shown in Figure 1. In the ^2A state, the doubly occupied $6b_1$ orbital is weakly bonding at the planar structure. Thus, this state has a minimum at a nearly planar geometry with twist angle of only 16.7°. The $7a$ orbital, doubly occupied in the $^2B_1$ state of $[TME]^-$, is weakly bonding at perpendicular structure. Hence, the $^2B_1$ state has a D_{2d} equilibrium geometry. The $^2B_1$ state is 3 kcal/mol more stable than the ^2A state. This stability difference is again attributable to steric repulsion between the two allyl fragments. Thus, the CCC allyl angle in $^2B_1$ state opens from 119.3° for the D_{2h} structure to 126.5° for the D_{2d} structure (see Figure 3c).

The vibrational frequencies and zero-point vibrational energies (ZPEs) were calculated using REKS and ROKS methods for all stationary points on the torsional curves of the ^1A and $^3B_1$ states of TME and $^2B_1$ and ^2A states of $[TME]^-$. The ZPEs are 71.4, 69.5, 66.6, and 67.7 kcal/mol for the ^1A, $^3B_1$, $^2B_1$, and ^2A states, respectively. With these ZPEs, the energy gaps between the equilibrium structures of ^1A and $^3B_1$ states of TME and $^2B_1$ and ^2A states of $[TME]^-$ are 0.2 and 4.1 kcal/mol, respectively.

Let us consider now the implications of the present density functional and CASMP2 calculations on the gas-phase photoelectron spectroscopic results[9] and the findings of the matrix isolation ESR experiments.[2] The sizable energy gap between states of $[TME]^-$ implies that under the conditions of gas-phase experiment the lowest state, $^2B_1$, should be primarily populated and the photoelectron spectrum will arise from TME $\tilde{a}\ ^3B_1 \leftarrow [TME]^-\ \tilde{X}\ ^2B_1$ and TME $\tilde{X}\ ^1A \leftarrow [TME]^-\ \tilde{X}\ ^2B_1$ transitions.[9] Most likely, the transitions occur from the ground vibronic level of the $^2B_1$ state to the ground vibronic level of the ^1A state (which has also D_{2d} structure) and to the torsionally excited vibronic state of triplet TME. From the ROKS/BLYP/6-311G** calculations, the frequency of the torsional mode in $^3B_1$ TME equals 87 cm^{-1}, such that transition can occur to torsionally excited states with vibrational quantum number $n_{tors} \sim 5-6$. These results are compatible with the analysis given previously.[9]

In addition to torsional excitation, in both states of TME, the symmetric scissoring mode should be excited,[9] given the modest difference in the allylic CCC angles in $[TME]^-$ (126.5°) and in singlet (124.2°) and triplet (122.0°) TME. The frequencies of the symmetric scissoring mode calculated by the ROKS/BLYP/6-311G** method for the $^3B_1$ state and by the REKS/BLYP/6-311G** method for the ^1A state are 357.1 and 357.8 cm^{-1}, respectively. Next to these modes are vibrations corresponding to the tilting motions of the allylic fragments, at frequencies of 290.5 and 286.7 cm^{-1} for the $^3B_1$ and ^1A state, respectively, and antisymmetric scissoring modes at frequencies of 460.9 and 466.7 cm^{-1} for the $^3B_1$ and ^1A state, respectively.

The results of our vibrational analysis are in a reasonably good agreement with the experimental finding[9] that in photoelectron spectra of $[TME]^-$ the active vibrational modes with equal frequencies of 335 cm^{-1} are excited in the transitions to both states. Thus, the present result confirms the previous assignment[9] of the active vibrational modes to symmetric scissoring vibrations. Recall, however, that unlike the present REKS/ROKS results previous ab initio calculations[9] failed to yield equal frequencies for the suspected vibrational modes.

From the density functional calculations (with ZPEs taken into account), the transition from the $^2B_1$ state of $[TME]^-$ to the ^1A state of TME occurs at the energy of 0.929 eV and to the $^3B_1$ state at the energy of 0.991 eV. The latter result is in good agreement with the experimentally measured[9] 0.985 ± 0.01 eV energy for the TME $\tilde{a}\ ^3B_1 \leftarrow [TME]^-\ \tilde{X}\ ^2B_1$ transition. The calculated energy for the TME $\tilde{X}\ ^1A \leftarrow [TME]^-\ \tilde{X}\ ^2B_1$ transition is 0.074 eV larger than the experimentally measured[9] quantity, 0.855 ± 0.01 eV. The separation between the singlet and triplet peaks in the photoelectron spectrum of $[TME]^-$ is calculated to be 0.062 eV or 1.4 kcal/mol, whereas the experimental value[9] is 0.13 ± 0.01 eV or 3.0 ± 0.3 kcal/mol. These results indicate that the REKS/BLYP/6-311G** calculation underestimates somewhat the stability of the singlet state of TME. However, bearing in mind the accuracy provided by modern approximate density functionals,[12,14] this underestimation of 1.6 kcal/mol seems acceptable.

At the optimal triplet geometry, the ^1A and $^3B_1$ electronic states of TME are nearly degenerate. Difference in their electronic energies consists of only 0.04 kcal/mol in favor of singlet. However, adding the ZPEs makes the S−T gap −1.91 kcal/mol in favor of the triplet state. Even if the CASMP2 electronic energies are used instead of density functional energies, the S−T gap remains negative and amounts to −0.92 kcal/mol. Thus, transition from the ground state vibrational level of the triplet TME to torsionally excited vibrational level of the singlet TME seems quite unlikely at low $(16-65K)^2$ temperatures owing to energetic arguments.

Furthermore, relaxation of the $^3B_1$ state to the ^1A state should be extremely slow because of very small spin−orbit coupling between these states. Indeed, the SOC between these states should be zero due to symmetry for planar and perpendicular structures.[30] For the D_2 structures the SOC is allowed, but should

be very small, because at intermediate twists the $^3B_1$ state is covalent and ^1A is almost purely covalent. The SOC between covalent diradicaloid states is known to vanish.[30−32] And finally, electrons in the $6b_1$ and $7a$ orbitals are localized mostly on the terminal carbon atoms in TME. Thus, the matrix element of the spin−orbit operator which involves these orbitals can hardly be expected to have a sizable value. We calculated the SOC matrix elements between the $^3B_1$ and ^1A states using the (6,6)CASSCF/6-311G** wave function and triplet state geometries from ROKS optimization, and these elements appeared to be less than 0.05 cm^{-1}. The results of the SOC calculations are plotted in Figure 5. Consequently, because of extremely weak spin−orbit coupling and energetic preference for the triplet state at the triplet optimal structure, this state of TME should be metastable at low temperatures. This explains why a linear Curie−Weiss plot for temperature dependence of intensity of ESR signal was observed[2] in matrix isolation experiments, even though TME has a singlet ground state.

4. Conclusions

Density functional calculations indicate that the ground state of TME in the gas phase is the singlet ^1A state (D_{2d} molecular structure) with the triplet $^3B_1$ state (D_2 structure) being ca. 0.2 kcal/mol above. Comparison of the calculated transition energies in the photoelectron spectra of $[TME]^-$ anion, which correspond to the TME $\tilde{X}\ ^1A \leftarrow [TME]^-\ \tilde{X}\ ^2B_1$ and TME $\tilde{a}\ ^3B_1 \leftarrow [TME]^-\ \tilde{X}\ ^2B_1$ transitions, with the experimental data[9] shows that the stability of the singlet state may be underestimated by density functional calculations by ca. 1.6 kcal/mol. Thus, the previously given[9] assessment of the gas-phase singlet−triplet gap in TME of ca. 2.0 kcal/mol seems reasonable.

Density functional calculations predict that, in the vibrational spectra of the two states of TME, the modes corresponding to symmetric scissoring vibrations should have nearly equal frequencies of 357.8 cm^{-1} (^1A state) and 357.1 cm^{-1} ($^3B_1$ state). These results are in reasonably good agreement with the experimental observation[9] of two modes of 335 cm^{-1} frequency in the vibrational structure of the photoelectron spectrum of $[TME]^-$ anion. Thus, the previously given[9] assignment of these modes to symmetric scissoring vibrations is confirmed. Recall, that previous ab initio calculations[9] did not yield equal frequencies for the suspected modes in vibrational spectra of singlet and triplet TME.

The present calculations confirm that matrix-isolated[2] TME does display triplet metastability. The $^3B_1$ state falls ca. 1−2 kcal/mol below the singlet state at the triplet optimal structure. Furthermore, the metastability of triplet state is guaranteed by extremely small spin−orbit coupling between the $^3B_1$ and ^1A states of TME. The spin−orbit matrix elements calculated with (6,6)CASSCF wave function at the triplet geometries from density functional optimizations are less than 0.05 cm^{-1} for all torsional angles considered. The probability of spin crossover estimated from the Landau−Zener[34,35] model with SOC matrix element $V_{SOC} = 0.05\ cm^{-1}$ and an excess energy $\Delta E_{excess} = 1$ kcal/mol is as small as 10^{-7}. Given the frequency of the torsional motion of the order of $10^{12}\ s^{-1}$ and a Boltzmann factor $\exp(-\Delta E_{excess}/RT)$, such a probability yields the lifetime of the triplet state of TME in the experimental[2] range of temperatures $T = 10-65$ K to vary in the limits from 10^{16} to 10^1 s.

Acknowledgment. The research is supported by the German−Israeli Foundation (GIF).

References and Notes

(1) Dowd, P. *J. Am. Chem. Soc.* **1970**, *92*, 1066.
(2) Dowd, P.; Chang, W.; Paik, Y. H. *J. Am. Chem. Soc.* **1986**, *108*, 7416.
(3) Borden, W. T. *J. Am. Chem. Soc.* **1975**, *97*, 5968.
(4) Borden, W. T.; Davidson, E. R. *J. Am. Chem. Soc.* **1977**, *99*, 4587.
(5) Berson, J. A. *Acc. Chem. Res.* **1997**, *30*, 238.
(6) Du, P.; Borden, W. T. *J. Am. Chem. Soc.* **1987**, *109*, 930.
(7) Nachtigall, P.; Jordan, K. D. *J. Am. Chem. Soc.* **1992**, *114*, 4743.
(8) Nachtigall, P.; Jordan, K. D. *J. Am. Chem. Soc.* **1993**, *115*, 270.
(9) Clifford, E. P.; Wenthold, P. G.; Lineberger, W. C.; Ellison, G. B.; Wang, C. X.; Grabowski, J. J.; Vila, F.; Jordan, K. D. *J. Chem. Soc., Perkin Trans. 2* **1998**, 1015.
(10) Borden, W. T.; Davidson, E. R. *Acc. Chem. Res.* **1996**, *29*, 67.
(11) Kohn, W.; Sham, L. J. *Phys. Rev.* **1965**, *140*, A1133.
(12) Parr, R. G.; Yang, W. *Density-Functional Theory of Atoms and Molecules*; Clarendon: Oxford, 1989.
(13) Dreizler, R. M.; Gross, E. K. U. *Density Functional Theory: an Approach to the Many-Body Problem*; Springer: Berlin, 1990.
(14) Johnson, B. G.; Gill, P. M. W.; Pople, J. A. *J. Chem. Phys.* **1992**, *97*, 7846.
(15) Gritsenko, O. V.; Schipper, P. R. T.; Baerends, E. J. *J. Chem. Phys.* **1997**, *107*, 5007.
(16) Neumann, R.; Nobes, R. H.; Handy, N. C. *Mol. Phys.* **1996**, *87*, 1.
(17) Gräfenstein, J.; Kraka, E.; Cremer, D. *Chem. Phys. Lett.* **1998**, *288*, 593.
(18) Cramer, C. J.; Nash, J. J.; Squires, R. R. *Chem. Phys. Lett.* **1997**, *277*, 311.
(19) Schreiner, P. R. *J. Am. Chem. Soc.* **1998**, *120*, 4184.
(20) Filatov, M.; Shaik, S. *Chem. Phys. Lett.* **1999**, *304*, 429.
(21) Hehre, W. J.; Radom, L.; Schleyer, P. v. R.; Pople, J. A. *Ab Initio Molecular Orbital Theory*; Wiley-Interscience: New York, 1986.
(22) Filatov, M.; Shaik, S. *Chem. Phys. Lett.* **1998**, *288*, 689.
(23) Filatov, M.; Shaik, S. *J. Chem. Phys.* **1999**, *110*, 116.
(24) Amos, R. D.; Alberts, I. L.; Andrews, J. S.; Collwell, S. M.; Handy, N. C.; Jayatilaka, D.; Knowles, P. J.; Kobayashi, R.; Koga, N.; Laidig, K. E.; Maslen, P. E.; Murray, C. W.; Rice, J. E.; Sanz, J.; Simandrias, E. D.; Stone, A. J.; Su, M.-D. *CADPAC5: The Cambridge Analytic Derivatives Package*; Cambridge: U.K., 1992.
(25) (a) Becke, A. D. *Phys. Rev. A* **1988**, *38*, 3098. (b) Lee, C.; Yang, W.; Parr, R. G. *Phys. Rev. B* **1988**, *37*, 785.
(26) Hirao, K. *Chem. Phys. Lett.* **1992**, *190*, 374.
(27) Nakano, H. *J. Chem. Phys.* **1993**, *99*, 7983.
(28) Schmidt, M. W.; Baldridge, K. K.; Boatz, J. A.; Elbert, S. T.; Gordon, M. S.; Jensen, J. H.; Koseki, S.; Matsunaga, N.; Nguyen, K. A.; Su, S. J.; Windus, T. L.; Dupuis, M.; Montgomery, J. A. *GAMESS-USA* (Rev. Feb. 1995).
(29) (a) Koseki, S.; Schmidt, M. W.; Gordon, M. S. *J. Phys. Chem.* **1992**, *96*, 10768. (b) Koseki, S.; Gordon, M. S.; Schmidt, M. W.; Matsunaga, N. *J. Phys. Chem.* **1995**, *99*, 12764.
(30) Danovich, D.; Marian, C. M.; Neuheuser, T.; Peyerimhoff, S. D.; Shaik, S. *J. Phys. Chem. A* **1998**, *102*, 5923.
(31) Salem, L.; Rowland, C. *Angew. Chem., Int. Ed. Engl.* **1972**, *11*, 92.
(32) Michl, J. *J. Am. Chem. Soc.* **1996**, *118*, 3568.
(33) For example, the REKS/BP86/6-31G* calculation does not yield the transition state in this region, rather a very flat potential curve which looks qualitatively exactly like what is presented here.
(34) Landau, L. D. *Phys. Z. Sowjetunion* **1932**, *2*, 46.
(35) Zener, C. *Proc. R. Soc. London Ser. AB* **1932**, *7*, 696.